

## Dynamics of a high- $Q$ vertical cavity organic laser

M. Koschorreck,\* R. Gehlhaar, V.G. Lyssenko, M. Swoboda, M. Hoffmann, and K. Leo  
*Institut für Angewandte Photophysik, Technische Universität Dresden, 01062 Dresden, Germany*

We investigate the dynamics of the organic laser guest-host composite of tris-(8-hydroxy quinoline) aluminium ( $\text{Alq}_3$ ) and 4-(dicyanomethylene)-2-methyl-6-(*p*-dimethylaminostyryl)-4H-pyran (DCM) embedded in a high- $Q$  ( $Q \approx 4500$ ) double distributed Bragg reflector microcavity (2DBR) using sub-picosecond up-conversion techniques. Lasing is observed at a threshold of  $0.4 \text{ nJ}/20 \mu\text{Jcm}^{-2}$  with a line-width of  $0.05 \text{ nm}$  (resolution limit). We observe a strongly nonlinear intensity-dependent delay of the emitted radiation burst. All experimental results are successfully modeled by a set of nonlinear rate equations, emphasizing the importance of a feedback mechanism for lasing.

Organic solid state lasers aim to combine the flexibility of organic materials with the technological advantages of a solid state light emitter, having the ultimate goal of electrical pumping [1, 2]. Optically pumped organic vertical cavity surface emitting lasers (VCSEL) were first demonstrated for polymers by Tessler *et al.* [4] and for small molecules by Bulovic *et al.* [3], the latter structure using the host-guest system of ( $\text{Alq}_3$ ) (tris-(8-hydroxy quinoline) aluminium) doped with the laser dye DCM (4-(dicyanomethylene)-2-methyl-6-(*p*-dimethylaminostyryl)-4H-pyran) as active medium [5]. Advantages are (i) the host efficiently absorbs the pump light and non-radiatively transfers it via a Förster process to the emitting DCM molecules with high efficiencies of up to 90% [6] (ii) the low concentration of emitters reduces bimolecular annihilation and thus lowers the laser threshold. Since then, lasing and amplified spontaneous emission in these material combinations have been observed in many geometries [7–9] and compound mixtures [10, 11].

Here, we investigate the threshold behavior and ultrafast dynamics of an organic  $\text{Alq}_3$ :DCM VCSEL optically pumped with sub-picosecond pulses. In contrast to previous organic VCSEL [3, 4] with a metal top mirror, we use distributed Bragg reflectors (DBR) for both mirrors, resulting in high  $Q$ -factors (up to 4500). These high  $Q$ -factors are also in contrast to the polymer microcavity laser in Ref. [12], where two mirrors were pressed together. By pumping with ultra-short pulses and detection by upconversion, we obtain a laser emission burst with particularly simple dynamics that can be fully described by standard laser rate equations, comparable to the analysis of the mirror-less geometry in Ref. [8]. Our device shows a dramatic threshold behavior, with the output intensity jumping by 4 orders of magnitude. The high  $Q$  factor and the sub-picosecond optical pump pulses avoid relaxation oscillations [3, 21] and thus allow a complete modeling of the emission dynamics in an organic VCSEL. The emitted light is radiated in a cone perpendicular to the surface with an angle

of a few degrees, which increases with pump intensity.

Our device is sketched in Fig. 1. The dielectric mirrors consisting of alternating layers of  $\text{SiO}_2$  and  $\text{TiO}_2$  are prepared by electron-beam deposition in high vacuum. The cavity is filled with a DCM doped layer of  $\text{Alq}_3$ , produced by thermal co-evaporation in the same vacuum system. The concentration of DCM was adjusted to be 2% by weight or  $N_D \approx 5 \times 10^{19} \text{ cm}^{-3}$  by volume to minimize the lasing threshold [13]. The linear transmission spectrum of this cavity (inset (a) of Fig. 2) shows two cavity modes at 624 nm and 711 nm, of which only the mode at 624 nm is sufficiently overlapping with the DCM emission spectrum to allow lasing. From optical modelling of the transmission spectrum, the thickness of the cavity is derived to be  $670 \text{ nm}$  corresponding to  $3.7\lambda/2$  at  $\lambda = 624 \text{ nm}$ . A high resolution transmission spectrum of the cavity mode (measured with a spot size of  $\sim 20 \mu\text{m}$  using white light generated by the regenerative amplifier) is shown in inset (b) of Fig. 2. The spectral width corresponds to a  $Q$ -factor of 3500. This spectral width is still affected by a gradient in the layers; extrapolation to zero spot size implies a local  $Q$  of 4500. For laser emission, the microcavity was optically pumped by the frequency doubled output of a regenerative Ti:Sa amplifier (SPITFIRE, Spectra-Physics), providing pulse lengths of about 200 fs at a repetition rate of 1 kHz. All

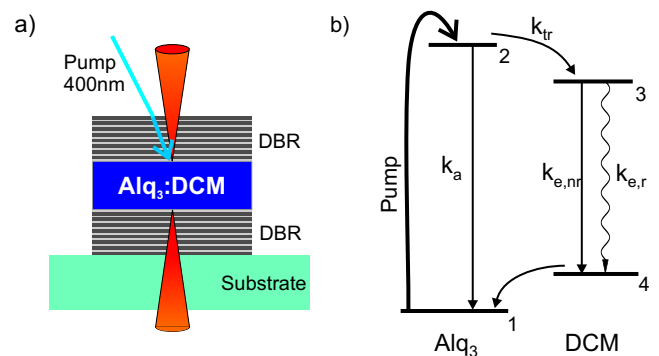


Figure 1: Left: Microcavity structure with an active layer of  $\text{Alq}_3$  : DCM. Right: The four-level scheme utilized for rate equation modelling. For the meaning of all symbols, see text.

\*Present address: ICFO - Institut de Ciències Fotòniques, Jordi Girona 29, Nexus II, 08034 - Barcelona, Spain; Electronic address: marco.koschorreck@icfo.es; URL: <http://www.icfo.es>

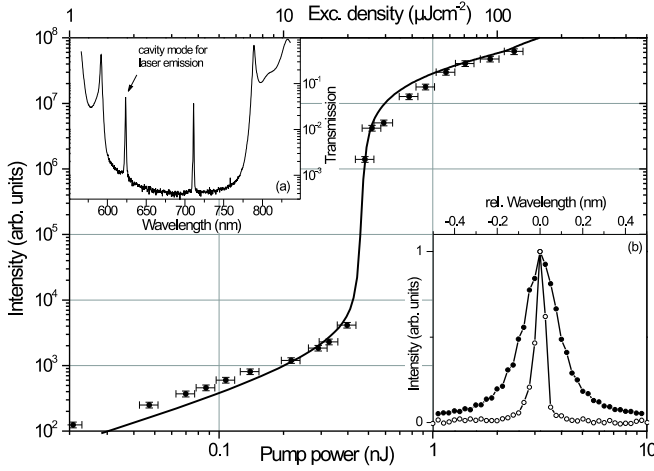


Figure 2: Input-output characteristics of the organic microcavity where the points are peak intensities of the spectral lines. The solid line displays the calculated characteristics. Inset a: linear transmission spectrum, for details see text. Inset b: transmission close to the cavity mode ( $-\bullet-$ ) and laser emission line above threshold ( $-\circ-$ ). Absolute positions are not comparable.

data are taken under ambient conditions.

In a first set of experiments, the emission spectra for different pump pulse intensities are measured. For this purpose, the conical laser emission was guided into a 750 nm monochromator with CCD-detector. At the pump wavelength of 400 nm, the microcavity has low reflection for a large range of incident angles. Hence, the fraction  $A$  of energy deposited in the microcavity is measured from reflection and transmission to be  $A = 1 - R - T = 90\%$ . From this fraction and the measured excitation spot size ( $50\ \mu\text{m}$ ), excitation densities are calculated. The recorded emission peak intensities vs. pump energy are plotted in Fig. 2. This plot shows a clear threshold at pulse energies of about  $20\ \mu\text{Jcm}^{-2}$  corresponding to excitation densities of  $5.5 \times 10^{17}\text{cm}^{-3}$ . The laser emission spectrum above threshold (inset (b) of Fig. 2) has a line-width of  $0.05\ \text{nm}$  limited by the set-up resolution.

The temporal dynamics are determined by an up-conversion setup, where the emission and a fraction of the amplifier output at  $\lambda = 800\ \text{nm}$  are overlapped in a  $200\ \mu\text{m}$  BBO crystal and the up-converted light is detected by a photomultiplier. The response function (FWHM =  $400\ \text{fs}$ ) is shown together with the measured emission traces in Fig. 3(a), showing that it can here be considered as delta function.

A set of VCSEL emission traces for pump intensities increasing from  $28\ \mu\text{J}/\text{cm}^2$  (just above threshold) to  $40\ \mu\text{J}/\text{cm}^2$  is shown in Fig. 3(a). Both delay and output pulse width strongly decrease with higher pumping, as it is well known for gain-switched semiconductor laser diodes [14, 15]. To evaluate the results, we apply a nonlinear rate equation approach similar to Ref. [14], assuming a four-level system appropriate for this guest-host composite: The  $\text{Alq}_3$  molecules absorb the blue pulses ( $1 \rightarrow 2$ ), this excitations reaches the DCM molecules via a Förster transfer ( $2 \rightarrow 3$ ), followed by photon emission ( $3 \rightarrow 4$ ).

Rate equations (1-3) describe the evolution of exciton population in the absorbing level 2 ( $N_a(t)$ ), in the emitting level 3 ( $N(t)$ ), and the photon density  $q(t)$ :

$$\frac{dN_a}{dt} = -k_a N_a(t) - k_{tr} N_a(t) \quad (1)$$

$$\frac{dN}{dt} = k_{tr} N_a(t) - k_e N(t) - c\sigma_{SE} q(t) N(t) \quad (2)$$

$$\frac{dq}{dt} = (c\Gamma\sigma_{SE} N(t) - k_{cav}) q(t) + \Gamma k_{e,r} \beta N(t) \quad (3)$$

Due to the delta-like pumping, the initial population in level 2 is  $N_{a,0} = A \frac{E_{pump}}{h\nu_{pump}} \frac{1}{V_{exc}}$ , which is the pulse energy divided by the photon energy and the excitation volume,  $V_{exc}$ . The factor  $A$  accounts for the fraction of absorbed light obtained above as  $A = 0.9$ .

The absorbing level 2 is depopulated by two processes. First, by radiative and non-radiative relaxations back to the ground state 1, described in the combined rate constant  $k_a$ . Considering that  $k_a \ll k_{tr}$ , we use the free space value  $(16\ \text{ns})^{-1}$  [16] as an approximation. The second term in Eq. (1) is the rate of energy transfer to laser level 3, i.e., the pumping rate of the lasing transition. Obviously, the dynamics of the laser are determined by a gain switching process that is not simply given by the delta-shaped optical pump pulse but rather by the finite timescale of the energy transfer constant  $k_{tr}$ , which will be treated as fit parameter. This treatment of energy transfer corresponds to Ref. [8], but neglecting satura-

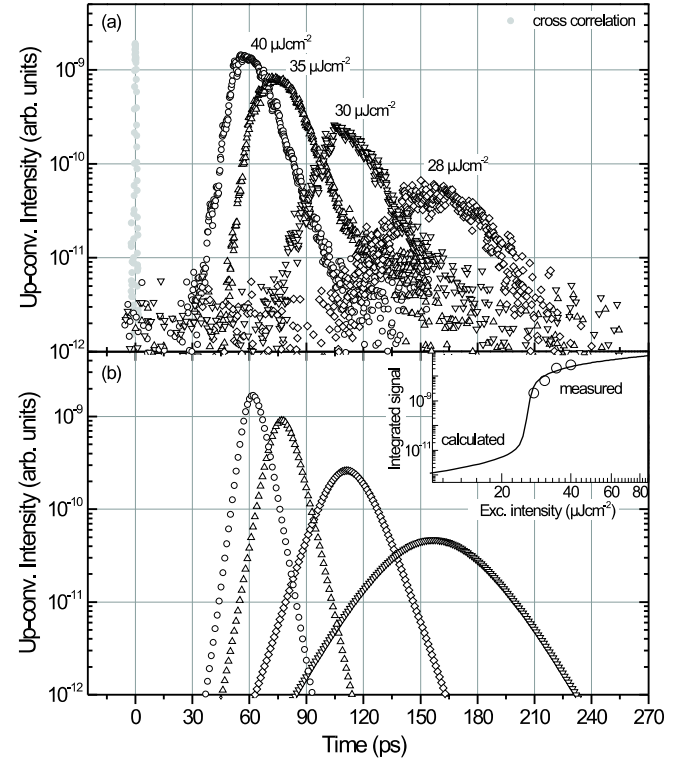


Figure 3: a) up-converted OVCSEL output b) Model calculations for the corresponding excitation densities

tion of level 3 in the rate equations which is well satisfied in our case, since the number of absorbed photons at threshold is much less (approximately 1%) than the number of emitter molecules.

Here, the population inversion is directly given by  $N(t)$  in Eq. (2). There, the first term is the pumping rate as described above. The two remaining terms account for the losses of population.  $k_e$  is the depopulation rate constant for all spontaneous processes, given by a sum  $k_e = k_{e,r} + k_{e,nr}$ . For the radiative lifetime  $k_{e,r}^{-1}$ , we use the free space value 5 ns [17]. The nonradiative rate constant  $k_{e,nr}$  is a fit parameter. The third term in Eq. (2) is the rate of stimulated decay of population, being proportional to the photon density  $q$ , inversion population  $N$  and the stimulated emission cross section  $\sigma_{SE}$ .  $c$  is the vacuum speed of light.

Rate equation (3) gives the change in photon density  $q$ . The first term is proportional to the number of stimulated emitted photons from Eq. (2) with the confinement factor  $\Gamma$  describing the spatial overlap of active medium and cavity mode. The second term includes all cavity losses with the rate constant  $k_{cav} = 1/\tau_{cav}$ . The cavity photon lifetime  $\tau_{cav}$  is calculated from  $Q = 2\pi\nu\tau_{cav}$ . The last term in Eq. (3) contains the spontaneous emission into the laser mode with  $\beta$  as fraction emitted into the laser mode.

We now simplify the analysis of the rate equations by rewriting them as follows: The solution of Eq. (1)  $N_a(t) = N_{a,0}e^{-(k_a+k_{tr})t}$  directly gives the pumping rate  $R(t) \equiv k_{tr}N_a(t)$  for the laser level. Furthermore, we rearrange terms in Eq. (2) and (3) by using the threshold density  $N_{thr} = \frac{k_{cav}}{c\Gamma\sigma_{SE}}$  [18], which can be directly obtained from the input-output characteristics in Fig. 2 (see above). Then, the rewritten equations read

$$\frac{dN}{dt} = R(t) - k_e N(t) - \frac{k_{cav}}{\Gamma} \frac{N(t)}{N_{thr}} q(t) \quad (4)$$

$$\frac{dq}{dt} = k_{cav} \left( \frac{N(t)}{N_{thr}} - 1 \right) q(t) + \Gamma k_{e,r} \beta N(t). \quad (5)$$

The equations are numerically solved by a fourth-order Runge-Kutta algorithm. There are four free parameters:  $k_{tr}$

(contained in  $R(t)$ ),  $k_e$ ,  $\Gamma$  and  $\beta$ . These were determined by two criteria (i) the input-output characteristic, seen in Fig. 2, are used to adjust  $\beta$  so that the s-shaped curve is fitted best, yielding  $\beta = 6 \times 10^{-4}$  (ii) the remaining three parameters were used to fit the up-conversion traces of Fig. 3, resulting in  $k_{tr}^{-1} = 19$  ps,  $\Gamma = 0.31$ , and  $k_e^{-1} = 1.3$  ns.

The emission dynamics observed in our experiments are closely related to the dynamics of amplified spontaneous emission from “free” layers (without resonator) of the same composite [8]. In contrast to Ref. [8], we do not observe relaxation oscillations since we work with resonator in a regime of lower excitation density and without saturating the emitting level. Hence, the host (Alq<sub>3</sub>) does not act as an energy reservoir and the emitting level is depleted by a single laser pulse. Interestingly, our Förster transfer rate deviates from the value  $k_{tr}^{-1} = 10$  ps reported for the “free” layer [8]. This behavior of inhibited energy transfer is explained [19, 20] by the absence of cavity modes in the spectral region of the transfer.

We now compare to the related organic VCSEL experiments with the same active material [3, 21]. There, the cavity consisted of a bottom DBR and a top silver mirror, yielding a  $Q$ -factor of 420 [21], which is consistent with the observed period of relaxation oscillations in [3]. Since we employ a high quality DBR also as top mirror, we reach an approximately tenfold higher  $Q$  and thus an approximately tenfold lower pump threshold ( $20 \mu\text{Jcm}^{-2}$  instead of  $300 \mu\text{Jcm}^{-2}$  [3]). Still, for electrical pumping our threshold would correspond to an injection current of  $j = \frac{2nek_e}{\chi} = 36 \text{ kAcm}^{-2}$ , with  $n$  as number of excitons formed in the composite layer,  $e$  the elementary charge and  $\chi = 1/4$  the fraction of radiative excitons. This high current density, together with additional loss mechanisms for electrical pumping, show that even an organic VCSEL with double DBR is far from an electrically pumped laser.

We are grateful to T. Fritz and H. Fröb for stimulating discussions. The authors acknowledge funding by the EU Commission through 5th framework Research Training Network ‘HYTEC’ (HPRN-CT-2002-00315) and by the Deutsche Forschungsgemeinschaft (Leibniz award).

- 
- [1] G. Kranzelbinder and G. Leising, Rep. Prog. Phys. **63**, 729 (2000)
- [2] M.A. Baldo and R.J. Holmes and S.R. Forrest, Phys. Rev. B **66**, 035321 (2002)
- [3] V. Bulovic, V.G. Kozlov, V.B. Khalifa and S.R. Forrest, Science **279**, 553 (1998)
- [4] N. Tessler, G.J. Denton and R.H. Friend, Nature **382**, 395 (1996)
- [5] V.G. Kozlov, V. Bulovic, P.E. Burrows and S.R. Forrest, Nature **389**, 362 (1997)
- [6] G.Y. Zhong, J. He and S.T. Zhang, Z. Xu, Z.H. Xiong, H.Z. Shi, X.M. Ding, W. Huang and X.Y. Hou, Appl. Phys. Lett. **80**, 4846 (2002)
- [7] M. Berggren, A. Dodabalapur and R.E. Slusher, Appl. Phys. Lett. **71**, 2230 (1997)
- [8] C. Kallinger, S. Riechel, O. Holderer, U. Lemmer, J. Feldmann, S. Berleb, A.G. Muckl and W. Brütting, J. Appl. Phys., **91**, 6367 (2002)
- [9] D. Schneider, S. Hartmann, T. Benstem, T. Dobbertin, D. Heithecker, D. Metzendorf, E. Becker, T. Riedl, H.H. Johannes, W. Kowalsky, T. Weimann, J. Wang and P. Hinze, Appl. Phys. B **77**, 399 (2003)
- [10] A. Dodabalapur, M. Berggren, R.E. Slusher, Z. Bao, A. Timko, P. Schiortino, E. Laskowski, H.E. Katz and O. Nalamasu, IEEE J. Sel. Topics Quant. Opt. **4**, 67 (1998)
- [11] V.G. Kozlov, G. Parthasarathy, P.E. Burrows, S.R. Forrest, Y. You and M.E. Thompson, Appl. Phys. Lett. **72**, 144 (1998)
- [12] T. Granlund, M. Theander, M. Berggren, M. Andersson, A. Ruzbeckas, V. Sundström, G. Björk, M. Granström, and O. Inganäs, Chem. Phys. Lett. **288**, 879 (1998)
- [13] V.G. Kozlov, V. Bulovic and S.R. Forrest, Appl. Phys. Lett. **71**, 2575 (1997)

- [14] M.S. Demokan and A. Nacaroglu, IEEE J. Quantum Electr. **20**, 1016 (1984)
- [15] L.G. Melcer, J.R. Karin, R. Nagarajan and J.E. Bowers, IEEE J. QuantumElectr. **27**, 1417 (1991)
- [16] C.W. Tang, S.A. VanSlyke and C.H. Chen, J. Appl. Phys. **85**,3610 (1989)
- [17] S.A. Kovalenko, N.P. Ernsting and J. Ruthmann, Chem. Phys. Lett. **258**, 445 (1996)
- [18] O. Svelto, *Principles of Lasers*, 4th ed. (Plenum Press, New York, 1998)
- [19] G.S. Agarwal and S.D. Gupta, Phys. Rev. A **57**, 667 (1998)
- [20] D.M. Basko, F. Bassani, G.C. La Rocca, V.M. Agranovich, Phys. Rev. B **62**, 15962 (2000)
- [21] V.G. Kozlov, V. Bulovic, P.E. Burrows, M. Baldo, V.B. Khalfi n, G. Parthasarathy, S.R. Forrest, Y. You and M.E. Thompson, J. Appl. Phys. **84**, 4096 (1998)